Biogeosciences Discuss., 7, 5157–5190, 2010
www.biogeosciences-discuss.net/7/5157/2010/
doi:10.5194/bgd-7-5157-2010

Biogeosciences Discussions

Coupling land surface and crop growth models for predicting evapotranspiration and carbon exchange in wheat-maize rotation croplands

H. Lei[1], D. Yang[1], E. Lokupitiya[2], and Y. Shen[3]

[1]State Key Laboratory of Hydroscience and Engineering, Department of Hydraulic Engineering, Tsinghua University, Beijing, 100084, China
[2]Department of Atmosphere Science, Colorado State University, Fort Collins, CO 80523, USA
[3]Key Laboratory of Agricultural Water Resources, Center for Agricultural Resources Research, Institute of Genetics and Developmental Biology, Chinese Academy of Science, Shijiazhuang, Hebei, 050021, China

Received: 26 May 2010 – Accepted: 25 June 2010 – Published: 2 July 2010

Correspondence to: D. Yang (yangdw@mail.tsinghua.edu.cn)

Published by Copernicus Publications on behalf of the European Geosciences Union.

Abstract

The North China Plain is one of the most important crop production regions in China. However, water resources in the area are limited. Accurate modeling of water consumption and crop production in response to the changing environment is important. To better describe the two-way interactions among climate, irrigation, and crop growth, the crop phenology and physiology scheme of the SiBcrop model was coupled with the Simple Biosphere model version 2 (SiB2) for simulating crop phenology, as well as the crop production and evapotranspiration of winter wheat and summer maize, two of the main crops in the region. In the coupled model, the Leaf Area Index (LAI) produced by the crop phenology and physiology scheme was used in estimating the sub-hourly energy and carbon fluxes. Observations obtained from two typical eddy covariance sites located in this region were used to validate the model. The coupled model was able to simulate carbon and energy fluxes, soil water content, biomass carbon, and crop yield with high accuracy, especially for the latent heat flux and carbon flux. The LAI was also well-simulated by the model. Therefore, the coupled model is capable of assessing the responses of water resources and crop production to the changes of future climate and irrigation schedules.

1 Introduction

The major crop production area in China is located in the northern area, particularly, in the Yellow River basin and the Haihe River basin. Northern China produces 59% of the national total crop production in 2008 (Ministry of Agriculture of China). Due to the semi-humid or arid climate, this region has limited water resources which are only 17% of the national total (Ministry of Water Resources of China). The problem between the large amount of water requirement for crop production and the limited availability of water resources is still an ongoing issue. In recent years, climate change (e.g., changes in precipitation, temperature, and CO_2 concentration [CO_2]) has drawn more

Discussion Paper | Discussion Paper | Discussion Paper | Discussion Paper |

BGD

7, 5157–5190, 2010

Coupling land surface and crop growth models

H. Lei et al.

attention on the potential impacts of this unresolved issue on future crop production. The effect of climate change and irrigation on crop production and water consumption is closely related with the food and water security of the nation. Thus, it is imperative for policy makers to address this concern.

Processes within the terrestrial ecosystem and atmosphere are intrinsically coupled. Environmental factors (e.g., water, temperature, and CO_2 concentration) control vegetation dynamics. Changes in vegetation, in turn, influence on water, energy, and carbon fluxes. Interactions and feedbacks among the climate, vegetation, and water have been significant concerns in recent years (Moorcroft, 2003; Kumar, 2007). Prescribing the vegetation phenology in terms of known values (e.g., leaf area index LAI) is the most common approach used by land surface models (Pitman, 2003). However, problems may be encountered if the model is set to make predictions because it does not describe a two-way feedback mechanism between vegetation and its ambient environment. Even though a model can be used with the prescribed LAI, the LAI derived from the Normalized Difference Vegetation Index (NDVI) which is based on remotely sensed information, may not capture the remarkable dynamics of the crops, thus, resulting in unsatisfactory magnitude and seasonality of carbon fluxes over croplands (Lokupitiya et al., 2009).

To date, many studies have coupled the vegetation dynamics model (crop growth model for agricultural ecosystem) with the land surface model for simulating water, energy, and carbon fluxes without prescribing crop phenology. Existing coupled models used for agricultural ecosystems are generally classified into three major classes, based on LAI calculation: A) LAI calculation is based on carbon allocation. Net accumulated assimilation calculated by the land surface model is allocated to different carbon pools. LAI is then calculated from the accumulated carbon in the leaf carbon pool (Boegh et al., 2004; Wang et al., 2007; Ivanov et al., 2008). B) LAI is directly calculated from bulk biomass, which is obtained from net assimilation calculated by the land surface model (Calvet et al., 1998). C) LAI is calculated from observed meteorological variables (e.g., temperature) and simulated variables (e.g., evapotranspiration

– ET, soil moisture, and soil temperature) from the land surface model (or the hydrological model) (Pauwels et al., 2007; Casanova and Judge, 2008; Maruyama and Kuwagata, 2010). The models in class C do not include the carbon processes, which limits their application for changing atmospheric [CO_2]. Although the models in class B include carbon simulation, production and other components relevant to crops are not simulated, limiting its application for crop production studies. In the models in class A, simulation of crop production, LAI, water-energy flux, and carbon flux are included, which, in turn, allows for wide applicability and comprehensive evaluation of the model with observations.

Following the models in class A, the Simple Biosphere model version 2 (SiB2, Sellers et al., 1996a,b) was coupled with the phenology and physiology scheme in the SiBcrop model (Lokupitiya et al., 2009) for simulating land-atmosphere exchanges relevant to two typical crops (winter wheat and maize) in the North China Plain. Winter wheat and maize production in this region accounts for 80 and 83% of the nation's winter wheat and maize production, respectively (Ministry of Agriculture of China). Compared with the previous similar study (Lokupitiya et al., 2009), this study mainly focuses on enabling the continuous modeling of ET and carbon flux in the North China Plain as well as its predictability in relation to climate change. Therefore, two eddy covariance (EC) sites with comprehensive observations were selected for evaluating the performance of the model. Sensitivity analyses were also conducted to test the behavior of the model under different irrigation amounts and [CO_2].

2 Description of the model

The SiB2 (Sellers et al., 1996a,b) was coupled with the carbon allocation-based crop phenology and physiology scheme of the SiBcrop model (Lokupitiya et al., 2009). The SiBcrop model has been applied in an annual winter wheat (growing season: November to June) field and an annual corn (growing season: May to August) field in the US. It resulted in a substantial improvement of the prediction of carbon exchange,

BGD
7, 5157–5190, 2010

compared with the original SiB, which uses remotely-sensed NDVI as input (Lokupitiya et al., 2009). In the coupled model, the SiB2-based daily total photosynthetic carbon assimilation, daily average soil water content (SWC), and air temperature are used within the crop phenology and physiology scheme to calculate the daily LAI which influences energy, water, and carbon dioxide exchange between the land surface and the atmosphere. Crop growth was assumed to not have been limited by nutrient availability because sufficient fertilizers were applied by the farmers.

2.1 Simple Biosphere model version 2

The SiB2 is a widely used land surface model for modeling energy, water, momentum, and carbon dioxide exchange between the land surface and the atmosphere. Comprehensive measurements were observed in the evaluation of the model at a number of sites (e.g., Baker et al., 2003; Gao et al., 2004; Hanan et al., 2005). The SiB2 simulated leaf carbon assimilation with C3 or C4 photosynthetic models (Farquhar et al., 1980; Collotz et al., 1991). Transpiration (Tr) was linked with leaf carbon assimilation by a stomatal conductance model (Ball et al., 1987). Fluxes were simulated in the electrical analog form which is expressed by multiplying the potential difference (i.e., vapor pressure, temperature, and CO_2 partial pressure gradients) with the conductance (i.e., aerodynamic, bare soil surface, and stomatal conductance). Heat transport in the soil was simulated by the force-restore model, which only simulates ground surface temperature and deep soil temperature. Further improvements to SiB2 in our study included the replacement of the soil hydrology model using the van Genuchten equation (Yang et al., 2000; Wang et al., 2009) and modifying certain parameters to tally with SiBcrop.

The input of the SiB2 consists of basic meteorological elements, such as downward short-wave radiation, downward long-wave radiation, relative humidity, air temperature, wind speed, air pressure, ambient [CO_2], and precipitation (and irrigation). In the SiB2, the world's land cover types were lumped into nine classes. The invariant properties of each class were assigned to values based on an extensive survey of ecological literature. The dynamics of vegetation were represented by variations in leaf area indexes (including total leaf area index and green leaf area index) and vegetation cover, which were all derived from remote-sensing NDVI through the relationship between LAI and the fraction of photosynthetically active radiation (PAR) absorbed by the green vegetation canopy (FPAR) and the simple ratio (SR, SR=(1+NDVI)/(1−NDVI)) (Sellers et al., 1996b). The soil physical parameters were from the measured soil water retention curve.

2.2 Crop phenology and physiology scheme based on the SiBcrop model

Crop emergency and subsequent growth stages were set based on the accumulated growing degree days (Lokupitiya et al., 2009). The growth rate during the initial seedling phase was determined by the amount of carbon stored in the seeds. Relevant further details could be found in Lokupitiya et al. (2009).

Because the planting dates were generally fixed, the planting dates of winter wheat and summer maize were artificially set as 10 October and 15 June, according to the general cropping system. Harvest dates were determined by the minimum of total requirements of the growing degree days and the planting dates of the next crop. The total biomass carbon, which is based on the daily photosynthetic assimilation calculated by the SiB2, was allocated to each carbon pool (roots, leaves, stems, and products) based on the phenology and physiology scheme. Because of the differences of climate and cropping pattern, the daily carbon allocation fractions of winter wheat and summer maize under unlimited water conditions were modified based on the experimental results in the North China Plain (Zhang et al., 2002; Qiao et al., 2002), and set by the growing degree days (Fig. 1). Compared to the original allocation scheme of maize in the SiBcrop, the new scheme was similar but had a slightly higher allocation fraction of leaves. Taking into account the impact of soil water stress on carbon allocation, this new allocation scheme was then revised based on the premise that it is advantageous for the plant to allocate carbon to the roots when soil moisture is limited (Arora and Boer, 2005), which is expressed as:

BGD
7, 5157–5190, 2010

$$\alpha_R = \frac{\varepsilon_R + \omega(1-W)}{1+\omega(1-W)} \quad (1)$$

$$\alpha_L = \frac{\varepsilon_L}{1+\omega(1-W)} \quad (2)$$

$$\alpha_S = \frac{\varepsilon_S}{1+\omega(1-W)} \quad (3)$$

$$\alpha_P = \frac{\varepsilon_P}{1+\omega(1-W)} = 1 - \alpha_R - \alpha_L - \alpha_S \quad (4)$$

where α_R, α_L, α_S, and α_P are the revised carbon allocation fractions for roots, leaves, stems, and products, respectively; ε_R, ε_L, ε_S, and ε_P are carbon allocation fractions under unlimited water conditions for roots, leaves, stems, and products, respectively; ω is set to be 0.8 for crops (Arora and Boer, 2005); W is the water availability in the root zone and is measured by:

$$W = \max\left[0, \min\left(1, \frac{\theta - \theta_r}{\theta^* - \theta_r}\right)\right] \quad (5)$$

where, θ is the volumetric soil water content in the root-zone, θ^* and θ_r are the threshold of incipient soil water stress and wilting point (see Table 1), respectively.

At the end of each day, the carbon in each pool was estimated by subtracting the growth and maintenance respiration from the daily biomass carbon allocation of each pool. Cumulative carbon in the leaf pool was then used to calculate the daily LAI, following details given in Lokupitiya et al. (2009). Parameters used in the coupled model correspond to default values in SiB2 and the SiBcrop models. Certain parameters were specific to the particular sites (Table 1).

3 Study area and measurements

The performance of the coupled model was evaluated by comparing observations and simulations at two EC flux tower sites in the North China Plain: Weishan site and Luancheng site. Both sites had irrigated winter wheat and rain-fed summer maize (irrigated in dry years), which were cultivated in rotation and typical in this region. The growing season of winter wheat is usually from October to June (dry season), and the growing season of summer maize is usually from June to October (rainy season). Comparing to the study of Lokupitiya et al. (2009), the growing season of wheat was similar while the growing season of maize was postponed for approximate one month.

The Weishan site (116°3′ E, 36°39′ N, 30 m a.s.l.) was located at the central North China Plain. The mean annual precipitation at the site was 553 mm, and mean annual air temperature was 13.8 °C. Mean annual pan (Φ20 cm) evaporation was 1950 mm. The groundwater table level ranged from 1.0 to 3.5 m within one year. The measurements consisted of meteorological measurements (i.e., precipitation, air temperature, relative humidity, wind speed, shortwave, longwave, and net radiation R_n), EC measurements (i.e., latent heat LE and sensible heat fluxes H_s, carbon dioxide exchange), underground measurements (i.e., soil heat flux G, soil temperature and moisture content profile), and LAI measurement (Table 2, see Lei and Yang, 2010a for details). As for the carbon flux, the observed net ecosystem exchange (NEE) was separated into the gross primary production (GPP) and ecosystem respiration (Lei and Yang, 2010b) for direct comparison with the simulated GPP. A Large Aperture Scintillometer (LAS) was installed, and the flux tower is in the middle of its path. A previous study showed that there was a satisfactory agreement between the sensible heat fluxes observed by LAS and EC technique at this relatively homogeneous landscape, indicating the high reliability of the sensible heat flux measurement (Yang et al., 2010). The observed sensible heat flux by the EC technique will be used for evaluating the model. The Luancheng site is located to the northwest of the Weishan site (114°41′ E, 37°53′ N, 50 m a.s.l.). Mean annual precipitation was 485 mm, and mean annual air temperature was

BGD
7, 5157–5190, 2010

12.8 °C. Mean annual pan (Φ20 cm) evaporation was 1616 mm. The groundwater table level was deeper than 30 m because of well irrigation. Measurements and instruments used were similar to those at the Weishan site. These are summarized in Table 2. Eddy covariance fluxes were adjusted for variations in air density due to the transfer of water vapor and sensible heat (Webb et al., 1980). Meteorological data, including air temperature, relative humidity, wind speed, and precipitation, were obtained from the national standard weather station at the site.

At both sites, LAI was estimated by measuring randomly sampled leaf areas from the field. Each sample included about ten plants of wheat or three plants of maize. The leaf area was measured using the area meter. Plant density was simultaneously recorded. The LAI was non-destructively measured using the LAI-2000 plant canopy analyze, starting from the maize season in 2008. In addition, dry weights of leaves, stems, and products (a plant other than root, leaf, and stem) at the Luancheng site were measured once a week. Two NDVI datasets, including eight-day/250 m resolutions and monthly/1 km resolution products, were obtained from the MODIS/Terra and used with algorithms in Sellers et al. (1996b) for deriving LAI, for comparison against the LAI produced by the coupled model. A filter was used as the noise-reduction technique to reduce noise in the NDVI time series (Velleman, 1980).

4 Model running

Vegetation type 9 (i.e., agriculture or C3 grassland) in the SiB2 and vegetation type 6 (i.e., C4 groundcover) were chosen to represent wheat and maize, respectively. Due to data availability, we ran the coupled model from 1 October 2007 to 30 September 2008 hourly at the Luancheng site. This period included one whole winter wheat season and one whole summer maize season. Hourly observed energy, water, and carbon dioxide fluxes, LAI, and dry biomass were compared with the values predicted by the model. At the Weishan site, the coupled model was run half-hourly from 1 June 2005 to 8 June 2009. This simulation period included four winter wheat seasons and four summer

BGD
7, 5157–5190, 2010

maize seasons. Half-hourly observed energy, water, carbon dioxide fluxes, and LAI were compared with values predicted by the model. Two commonly used statistics (i.e., coefficient of determination – R^2 – for linear regression and root mean square error RMSE) were used to evaluate the model.

Once the coupled model was validated for present conditions, we tested the ability to use the model to simulate the crop yield and ET in different irrigation and [CO_2] situations. In Sect. 5.3, a sensitivity study is presented concerning the impact of the irrigation amount, but not of irrigation strategies. We chose the Luancheng site as case study, and the 2007–2008 wheat season was selected because there was no irrigation in the 2008 maize season. In this season, accumulated precipitation was 197 mm (mean seasonal precipitation was 130 mm) with an exceedance probability of about 11% (Sun et al., 2009), indicating that the season was relatively wet. Therefore, irrigation was implemented once with 122 mm in 4 April 2008, which was in the jointing stage of wheat. In Sect. 5.4, a sensitivity analysis was made with values of [CO_2] corresponding to 3×381, 2×381, and 381 ppm (i.e., the current level) at the Luancheng site from October 2007 to September 2008, assuming that other climate forcing data (e.g., air temperature) were kept as the same as the current situation. We wish to point out that our model only considered the responses of photosynthesis and leaf conductance to increased [CO_2], but was not able to simulate the response of carbon allocation to CO_2 enrichment because its underlying mechanism was not yet fully understood (Monje and Bugbee, 1998; Niklaus et al., 2001; Suter et al., 2002).

5 Results and discussion

5.1 Validation of the crop growth simulation

The coupled model was able to closely simulate LAI and biomass carbon, comparing to the observations at the two sites. The interannual variation of LAI was well simulated by the model (Figs. 2 and 3a). In contrast, the MODIS NDVI-based LAI was unsatifactory

BGD
7, 5157–5190, 2010

in reflecting the interannual variability of LAI, because it was saturated by its maximum values in the algorithms. The seasonal variability of wheat LAI was well simulated by both the eight-day NDVI and the coupled model, which resulted in high R^2 and low RMSE (Table 3). However, seasonal variability of maize LAI was unsatisfactorily simulated by NDVI, but was much better simulated by the coupled model (Table 3). These were essentially due to the fact that either NDVI or SR is generally insensitive to LAI when it exceeds a certain value (Gitelson et al., 2003; Sellers et al., 1996). The 1 km/monthly NDVI-based LAI had much lower peak value and was worse synchronous with the observed LAI (Fig. 2). This could be attributed to the interpolation scheme from monthly to daily values. Note that the predicted LAI by the model was much higher than the observed LAI in the 2008 maize season and the 2008–2009 wheat season, which could be attributed to the under-measurement of LAI by LAI-2000 in row crops due to sampling (Wilhelm et al., 2000).

By converting the measured dry biomass to biomass carbon (by multiplying 0.45 for the product and 0.5 for the stem and leaf), we compared the simulated and observed carbon biomass for different pools at the Luancheng site (Fig. 3). The simulations and measurements agreed quite well over the whole growing season for both wheat and maize. The square of the Pearson product-moment correlation coefficient (r^2) ranged from 0.81 to 0.98. The simulated ratio of root biomass to above-ground biomass was 0.14 and 0.08 for wheat and maize, respectively. These values were acceptable compared to the common values (0.15–0.20 for wheat and 0.10–0.15 for maize) in this region (Mo et al., 2005).

5.2 Validation of the surface fluxes simulation

The seasonal variation in simulated and observed values of energy fluxes (R_n, LE, H_s, and G), NEE, and SWC for the Weishan and Luancheng sites are shown in Figs. 4 and 5, respectively. Table 4 lists the statistics of the comparisons. The seasonal variation in surface fluxes and SWC showed good agreement between the simulated and observed values. The R_n simulation had the highest R^2 and lowest RMSE. Simulated

NEE and LE had the second highest R^2. Overall, the R^2 of NEE and LE were all greater than 0.7 in the whole seasons, which indicated that the model could explain more than 70% of the variability in the observed latent and carbon dioxide fluxes. The results suggest that the model is sound in simulating latent heat and carbon fluxes in this region. The simulation of carbon flux can also be confirmed by the comparison of the simulated GPP and observation-derived GPP at the Weishan site (Fig. 6), which excluded the influence of soil respiration modeling. At the Luancheng site, the simulated seasonal soil evaporation total accounted for 32% of the simulated seasonal ET total in the wheat season, and the ratio of simulated seasonal total soil evaporation of simulated seasonal total ET was 35% for the maize season. The ratios were acceptable but higher, comparing to the observed values of 29.7% for wheat seasons and 30.3% for maize seasons at the Luancheng site averaged from 1995 to 2000 (Liu et al., 2002). Relatively high RMSE and low R^2 were found for the sensible heat flux. The seasonal variation in simulated soil heat flux was asynchronous with the observed soil heat flux, which could be explained by the mismatch between the simulated ground surface heat flux and measured soil heat flux in the depth of 3 cm (Shao et al., 2008).

5.3 Comparison with the original SiB2

For comparison, the results for LE and NEE simulated by the original SiB2 given eight-day and monthly NDVI as input were compared with the results of the coupled model, respectively. The R^2, RMSE and slope of linear regression (β) values for the overall comparisons were listed in Table 5. For NEE, the coupled model is the most accurate, whereas the SiB2 with a monthly NDVI is the least accurate. This was similar to the work of Lokupitiya et al. (2009). However, there were no significant differences among the results for LE in the overall comparison. Figure 7 shows the daily course of midday-averaged LE at a selected period. Although the peak LAI was much under-estimated by the monthly NDVI, no significant differences were found between LE resulted from the coupled model and the original SiB2 with a monthly NDVI. However, the ratio of

BGD
7, 5157–5190, 2010

transpiration to ET decreased from 51% to 46% when the coupled model was replaced with the original SiB2, implying that the original SiB2 may over-predict soil evaporation.

5.4 Sensitivity to irrigation amount

Figure 8 shows the simulated SWC in the root-zone in different irrigation amounts. By converting the biomass carbon in the products (by multiplying by 2.2) to biomass and considering a water content of about 14% in the wheat kernel, we estimated approximately the crop yield which was listed in Table 6. In cases 6–7 and in reality, the wheat growth was not stressed by soil water because the average SWC was above $0.22\,m^3\,m^{-3}$ at any time in the season. Excess irrigation did not lead to a further increase in ET, Tr, and yield (Table 6), but it percolated into the deeper soil and/or drained as surface runoff. In cases 3–5, soil water stress occurred in the milking stage of wheat, leading to a reduction in ET, Tr, and yield. However, the maximum LAI was slightly reduced because the canopy had been fully developed before the milking stage. In cases 1 and 2, wheat was under moderate soil water stress through jointing stage and flowering stage until maturity, respectively, which led to a significant decrease in ET, Tr, yield, and LAI. The simulated water use efficiency (defined as the ratio of crop yield to total ET) increased with the increase of the irrigation till irrigation reached 122 mm. A further increase in irrigation would not increase the water use efficiency, indicating a waste of water. The sensitivity study showed that the feedbacks among crop growth, ET, yield, and soil water can be reasonably described by the coupled model.

5.5 Sensitivity to CO_2 concentration

In the absence of soil water stress, the changes of ET and SWC with an increase in [CO_2] result from the trade-off between increased LAI (which was because of enhanced photosynthesis) and decreased leaf conductance (Calvet et al., 1998). Figure 9 presents the root-zone SWC under different prescribed values of [CO_2] at the Luancheng site. The corresponding seasonal summaries are listed in Table 7. The

BGD
7, 5157–5190, 2010

simulated SWC increased slightly in the wheat season, even though a significant increase in the LAI of wheat was observed because of CO_2 fertilization. This is because leaf stomatal closure limited the transpiration, which offset the positive feedback of transpiration to increased LAI. Simulated changes of SWC and ET in the maize season were similar to the results in the wheat season but corresponded to a slight increase in the LAI of maize. Simulated total biomass carbon of C3 wheat increased significantly by 42% under the doubled [CO_2] condition, but the relative change of total biomass carbon from doubled [CO_2] condition to tripled [CO_2] condition was significantly lesser. The simulated results were consistent with the experiments which showed that doubling [CO_2] from 350 to 700 ppm increased wheat yield by about 31%, but the effects of 1100–1250 ppm CO_2 on wheat yield were lesser than the effects of 600–700 ppm CO_2 (Amthor, 2001). On the other hand, both the LAI and the total biomass carbon of maize were unresponsive to the increased [CO_2] because CO_2 contributed nothing or little in the fertilization process of C4 maize, for the reason that the C4 photosynthesis is usually saturated at the current CO_2 concentration level (Leakey et al., 2006). The simulation results were similar with the modeling work on C3 crops and C4 maize from Calvet et al. (1998).

6 Conclusions

The crop phenology and physiology scheme in the SiBcrop model was coupled with the SiB2 model to estimate phenology, latent heat flux (i.e., ET), and carbon exchange in the winter wheat-summer maize rotation cropping fields in the North China Plain. Two typical EC flux sites with this cropping pattern were used to evaluate the performance of the model. The seasonal variations in carbon biomass, LAI, energy fluxes, carbon flux, and SWC showed good agreement with observed values. In particular, simulated latent heat flux and NEE explained the highest variability in their seasonal processes (R^2 for latent heat flux and carbon flux were greater than 0.7). Compared to the original SiB2 given remotely sensed NDVI as input, the coupled model improved the modeling

BGD
7, 5157–5190, 2010

of crop phenology and carbon flux, especially for the maize. The differences of seasonality of latent heat flux between the coupled model and the original SiB2 were not significant, but the SiB2 underestimated the proportion of transpiration to the total ET. Sensitivity analysis showed that the model was sensitive to the irrigation amount and atmospheric [CO_2], and gave reasonable results. Therefore, the coupled model is capable of simulating the response of ET and crop yield to different irrigation schedules and possible climate changes in this type of agro-ecosystem.

Acknowledgements. This research was supported by the National Natural Science Foundation of China (Project No. 50939004) and the National 973 Project of China (Project No. 2006CB403405).

References

Amthor, J. S.:. Effects of atmospheric CO_2 concentration on wheat yield: review of results from experiments using various approaches to control CO_2 concentration, Field Crop. Res., 73, 1–34, 2001.

Arora, V. K. and Boer, G. J.: A parameterization of leaf phenology for the terrestrial ecosystem component of climate models, Global Change Biol., 11, 39–59, 2005.

Baker, I., Denning, A. S., Hanan, N., Prihodko, L., Uliasz, M., Vidale, P.-L., Davis, K., and Bakwin, P.: Simulated and observed fluxes of sensible and latent heat and CO_2 at the WLEF-TV tower using SiB2.5, Global Change Biol., 9, 1262–1277, 2003.

Ball, J. T., Woodrow, I. E., and Berry, J. A.: A model predicting stomatal conductance and its contribution to the control of photosynthesis under different environmental conditions, in: Progress in Photosynthesis Research, edited by: Biggens, J., Martinus Nijhoff, Dordrecht, 221–224, 1987.

Boegh, E., Thorsen, M., and Butts, M. B.: Incorporating remote sensing data in physically based distributed agro-hydrological modeling, J. Hydrol., 287, 279–299, 2004.

Calvet, J., Noilhan, J., Roujean, J., Bessemoulin, P., Cabelguenne, M., Olioso, A., and Wigneron, J.: An interactive vegetation SVAT model tested against data from six contrasting sites, Agr. Forest Meteorol., 92, 73–95, 1998.

Casanova, J. J. and Judge, J.: Estimation of energy and moisture fluxes for dynamic

vegetation using coupled SVAT and crop-growth models, Water Resour. Res., 44, W07415, doi:10.1029/2007WR006503, 2008.
Collatz, G. J., Ribas-Carbo, M., and Ball, J. A.: Coupled photosynthesis – stomatal conductance model for leaves of C4 plants, Aust. J. Plant Physiol., 19, 519–538, 1992.
Farquhar, G. D., von Caemmerer, S., and Berry, J. A.: A biochemical model of photosynthetic CO_2 assimilation in leaves of C3 species, Planta, 149, 78–90, 1980.
Gao, Z., Chae, N., Kim, J., Hong, J., Choi, T., and Lee, H.: Modeling of surface energy partitioning, surface temperature, and soil wetness in the Tibetan prairie using the Simple Biosphere Model 2 (SiB2), J. Geophys. Res., 109, D06102, doi:10.1029/2003JD004089, 2004.
Gitelson, A. A., Viña, A., Arkebauer, T. J., Rundquist, D. C., Keydan, G., and Leavitt, B.: Remote estimation of leaf area index and green leaf biomass in maize canopies, Geophys. Res. Lett., 30(5), 1148, doi:10.1029/2002GL016450, 2003.
Hanan, N. P., Berry, J. A., Verma, S. B., Walter-Shea, E. A., Suyker, A. E., Burba, G. G., and Denning, A. S.: Testing a model of CO_2, water and energy exchange in Great Plains tallgrass prairie and wheat ecosystems, Agr. Forest Meteorol., 131, 162–179, 2005.
Ivanov, V. Y., Bras, R. L., and Vivoni, E. R.: Vegetation-hydrology dynamics in complex terrain of semiarid areas: 1. A mechanistic approach to modeling dynamic feedbacks, Water Resour. Res., 44, W03429, doi:10.1029/2006WR005588, 2008.
Kumar, P.: Variability, feedback, and cooperative process dynamics: elements of a unifying hydrologic theory, Geogr. Compass, 1(6), 1338–1360, 2007.
Leakey, A. D. B., Uribelarrea, M., Ainsworth, E. A., Naidu, S. L., Rogers, A., Ort, D. R., and Long, S. P.: Photosynthesis, productivity, and yield of maize are not affected by open-air elevation of CO_2 concentration in the absence of drought, Plant Physiol., 140, 779–790, 2006.
Lei, H.-M. and Yang, D.-W.: Interannual and seasonal variability in evapotranspiration and energy partitioning over an irrigated cropland in the North China Plain, Agr. Forest Meteorol., 158, 581–589, 2010a.
Lei, H.-M. and Yang, D.-W.: Seasonal and interannual variations in carbon dioxide exchange over a cropland in the North China Plain, Global Change Biol., in press, doi:10.1111/j.1365-2486.2009.02136.x, 2010b.
Liu, C., Zhang, X., and Zhang, Y.: Determination of daily evaporation and evapotranspiration of winter wheat and maize by large-scale weighing lysimeter and micro-lysimeter, Agr. Forest Meteorol., 111, 109–120, 2002.

Lokupitiya, E., Denning, S., Paustian, K., Baker, I., Schaefer, K., Verma, S., Meyers, T., Bernacchi, C. J., Suyker, A., and Fischer, M.: Incorporation of crop phenology in Simple Biosphere Model (SiBcrop) to improve land-atmosphere carbon exchanges from croplands, Biogeosciences, 6, 969–986, doi:10.5194/bg-6-969-2009, 2009.
Maruyama, A. and Kuwagata, T.: Coupling land surface and crop growth models to estimate the effects of changes in the growing season on energy balance and water use of rice paddies, Agr. Forest Meteorol., in press, doi:10.1016/j.agrforment.2010.02.011, 2010.
Ministry of Agriculture of China: http://www.moa.gov.cn/zwllm/sjzl/, last access: 15 April 2010.
Ministry of Water Resources of China: http://www.mwr.gov.cn/zwzc/hygb/szygb/qgszygb/201001/t20100119_171051.html, last access: 15 April 2010.
Mo, X., Liu, S., Lin, Z., Xu, Y., Xiang, Y., and McVicar, T. R.: Prediction of crop yield, water consumption and water use with a SVAT-crop growth model using remotely sensed data on the North China Plain, Ecol. Model., 183, 301–322, 2005.
Monje, O. and Bugbee, B.: Adaptation to high CO_2 concentration in an optimal environment: radiation capture, canopy quantum yield and carbon use efficiency, Plant Cell Environ., 21, 315–324, 1998.
Moorcroft, P. R.: Recent advances in ecosystem-atmosphere interactions: an ecological perspective, P. Roy. Soc. Lond. B. Bio., 270, 1215–1227, 2003.
Niklaus, P. A., Glöckler, E., Siegwolf, R., and Körner, C.: Carbon allocation in calcareous grassland under elevated CO_2: a combined ^{13}C pulse-labelling/soil physical fractionation study, Funct. Ecol., 15, 43–50, 2001.
Pauwels, V. R. N., Verhoest, N. E. C., De Lannoy, G. J. M., Guissard, V., Lucau, C., and Defourny, P.: Optimization of a coupled hydrology-crop growth model through the assimilation of observed soil moisture and leaf area index values using an ensemble Kalman filter, Water Resour. Res., 43, W04421, doi:10.1029/2006WR004942, 2007.
Pitman, A. J.: The evolution of, and revolution in, land surface schemes designed for climate models, Int. J. Climatol., 23, 479–510, 2003.
Qiao, Y., Yu, Z., and Driessen, P. M.: Quantification of dry matter accumulation and distribution among different organs of winter wheat, Chinese J. Appl. Ecol., 13(5), 543–546, 2002.
Sellers, P. J., Randall, D. A., Collatz, G. J., Berry, J. A., Field, C. B., Dazlich, D. A., Zhang, C., Collelo, G. D., and Bounoua, L.: A revised land surface parameterization (SiB2) for atmospheric GCMs, Part 1: Model formulation, J. Climatol., 9, 676–705, 1996a.
Sellers, P. J., Los, S. O., Tucker, C. J., Justice, C. O., Dazlich, D. A., Collatz, G. J., and

BGD
7, 5157–5190, 2010

Randall, D. A.: A revised land surface parameterization (SiB2) for atmospheric GCMs, Part 2: The generation of global fields of terrestrial biophysical parameters from satellite data, J. Climatol., 9, 706–737, 1996b.

Shao, C., Chen, J., Li, L., Xu, W., Chen, S., Gwen, T., Xu, J., and Zhang, W.: Spatial variability in soil heat flux at three Inner Mongolia steppe ecosystems, Agr. Forest Meteorol., 148, 1433–1443, 2008.

Shen, Y., Kondoh, A., Tang, C., Zhang, Y., Chen, J., Li, W., Sakura, Y., Liu, C., Tanaka, T., and Shimada, J.: Measurement and analysis of evapotranspiration and surface conductance of a wheat canopy, Hydrol. Process., 16, 2173–2187, 2002.

Sun, H., Shen, Y., Yu, Q., Flerchinger, G. N., Zhang, Y., Liu, C., and Zhang, X.: Effect of precipitation change on water balance and WUE of the winter wheat-summer maize rotation in the North China Plain, Agr. Water Manage., 97, 1139–1145, doi:10.1016/j.agwat.2009.06.004, 2009.

Suter, D., Frehner, M., Fischer, B. U., Nösberger, J., and Lüscher, A.: Elevated CO_2 increases carbon allocation to the roots of Lolium perenne under free-air CO_2 enrichment but not in a controlled environment, New Phytol., 154, 65–75, 2002.

Velleman, P. F.: Definition and comparison of robust nonlinear data smoothing algorithms, J. Am. Stat. Assoc., 75, 609–615, 1980.

Wang, L., Koike, T., Yang, K., Jackson, T. J., Bindlish, R., and Yang, D.: Development of a distributed biosphere hydrological model and its evaluation with the Southern Great Plains Experiments (SGP97 and SGP99), J. Geophys. Res., 114, D08107, doi:10.1029/2008JD010800, 2009.

Webb, E. K., Pearman, G. I., and Leuning, R.: Correction of the flux measurements for density effects due to heat and water vapour transfer, Q. J. Roy. Meteor. Soc., 106, 85–100, 1980.

Wilhelm, W. W., Ruwe, K., and Schlemmer, M. R.: Comparision of three leaf area index meters in a corn canopy, Crop Sci., 40, 1179–1183, 2000.

Yang, D., Chen, H., and Lei, H.: Estimation of evapotranspiration using a remote sensing model over agriculture land in the North China Plain, Int. J. Remote Sens., in press, 2010.

Yang, D., Herath, S., and Musiake, K.: Comparison of different distributed hydrological models for characterization of catchment spatial variability, Hydrol. Process., 14, 403–416, 2000.

Zhang, Y., Yu, Z., and Driessen, P. M.: Experimental study of assimilate production, partitioning and translocation among plant organs in summer maize (*Zea mays*) under various environmental and management conditions, Acta Agron. Hung., 28(1), 104–109, 2002.

Table 1. Site specific parameters used in the coupled model.

Symbol	Parameter	Value		Source
–	–	Weishan	Luancheng	–
θ^*	Threshold of incipient soil water stress ($m^3\,m^{-3}$)	0.22	0.22	Shen et al., 2002
θ_r	Wilting point ($m^3\,m^{-3}$)	0.12	0.13	measured
α	van Genuchten parameter (cm^{-1})	0.00483	0.0098	measured
n	van Genuchten parameter	1.99	2.18	measured

Discussion Paper | Discussion Paper | Discussion Paper | Discussion Paper |

BGD

7, 5157–5190, 2010

Coupling land surface and crop growth models

H. Lei et al.

Table 2. Summaries of the measurements and instruments.

Site	Observation items	Instruments	Height or depth
Weishan	Sensible and latent heat fluxes and carbon dioxide flux	CSAT3, Campbell Scientific, Inc., Logan, UT, USA and LI7500, LI-COR, Inc., Lincoln, NE, USA	3.7 m
	Downward (upward) shortwave (longwave) radiation	CNR-1, Kipp & Zonen, Delft, the Netherlands	3.5 m
	Soil heat flux	HFP01SC, Hukseflux, Delft, the Netherlands	−0.03 m
	Soil water content	TRIME-EZ/IT, IMKO, Ettlingen, Germany	−0.05, −0.1, −0.2, −0.4, −0.8, and −1.6 m
	Soil temperature	Campbell-107, Campbell Scientific Inc., Logan, UT, USA	−0.05, −0.1, −0.2, −0.4, −0.8, and −1.6 m
	Air temperature and relative humidity	HMP45C, Vaisala Inc., Helsinki, Finland	3.6 m
	Wind speed	05103, Young Co., 120 Traverse City, MI, USA	10.0 m
	Precipitation	TE525MM, Campbell Scientific Inc., 121 Logan, UT, USA	1.5 m
Luancheng	Sensible and latent heat fluxes and carbon dioxide flux	CSAT3, Campbell Scientific, Inc., Logan, UT, USA and LI7500, LI-COR, Inc., Lincoln, NE, USA	3.3 m
	Downward (upward) shortwave (longwave) radiation	CNR-1, Kipp & Zonen, Delft, the Netherlands	3.0 m
	Soil heat flux	HFP01, Hukseflux, Delft, the Netherlands	−0.02 m
	Soil water content	Neutron probe (IH-II, Institute of Hydrology, Wallingfoad, UK)	−0.1, −0.4, −0.6, and −1.0 m
	Soil temperature	105T, Campbell Scientific Inc., Logan, UT, USA	−0.02, −0.05, −0.1, −0.2, and −0.5 m
	Air temperature, relative humidity, wind speed, and precipitation	Chinese Meteorological Administration	1.5 m for air temperature and 10.0 m for wind speed

Table 3. Results of the comparisons of simulated and observed LAI. SiB2-8day was derived from eight-day NDVI and the SiB2-monthly was derived from monthly NDVI.

Site	period	R^2	RMSE
Weishan	Wheat season		
	Coupled model	0.80	0.98
	SiB2-8day	0.87	0.83
	SiB2-monthly	0.78	1.36
	Maize season		
	Coupled model	0.77	0.97
	SiB2-8day	0.63	1.31
	SiB2-monthly	0.36	1.59
Luancheng	Wheat season		
	Coupled model	0.75	1.35
	SiB2-8day	0.92	1.00
	SiB2-monthly	0.87	0.98
	Maize season		
	Coupled model	0.84	0.96
	SiB2-8day	0.75	1.21
	SiB2-monthly	0.43	1.70

BGD
7, 5157–5190, 2010

Table 4. Statistics for the comparisons against half-hourly observations at the Weishan site and hourly observations at the Luancheng site.

Variables	Site	Crop season	RMSE	R^2
Net radiation ($W\,m^{-2}$)	Weishan	Maize	14.5	0.99
		Wheat	14.5	1.0
	Luancheng	Maize	17.4	1.0
		Wheat	18.7	1.0
Latent heat flux ($W\,m^{-2}$)	Weishan	Maize	69.90	0.72
		Wheat	40.80	0.83
	Luancheng	Maize	45.50	0.84
		Wheat	35.6	0.85
Sensible heat flux ($W\,m^{-2}$)	Weishan	Maize	38.29	0.58
		Wheat	39.8	0.63
	Luancheng	Maize	30.18	0.68
		Wheat	32.64	0.57
Net ecosystem exchange ($\mu mol\,m^{-2}\,s^{-1}$)	Weishan	Maize	4.62	0.85
		Wheat	4.05	0.79
	Luancheng	Maize	5.58	0.82
		Wheat	4.73	0.78

BGD
7, 5157–5190, 2010

Table 5. Results for the comparisons of the coupled model and the original SiB2 using eight-day NDVI (SiB2-8day) and monthly NDVI (SiB2-monthly) as input. The wheat season was from 15 October to 14 June, and maize season was from 15 June to 14 October.

Variable	Site	Period	R^2	RMSE	β^*
Latent heat flux ($W\,m^{-2}$)	Weishan	Wheat season			
		Coupled model	0.83	40.8	0.89
		SiB2-8day	0.84	40.4	0.89
		SiB2-monthly	0.85	39.5	0.93
		Maize season			
		Coupled model	0.72	69.9	1.14
		SiB2-8day	0.73	61.6	1.08
		SiB2-monthly	0.69	69.5	1.10
	Luancheng	Wheat season			
		Coupled model	0.85	35.6	0.78
		SiB2-8day	0.76	44.9	0.67
		SiB2-monthly	0.85	36.0	0.76
		Maize season			
		Coupled model	0.84	45.5	1.01
		SiB2-8day	0.84	45.8	1.00
		SiB2-monthly	0.81	54.5	1.05
Net ecosystem exchange ($\mu mol\,m^{-2}\,s^{-1}$)	Weishan	Wheat season			
		Coupled model	0.79	4.1	0.91
		SiB2-8day	0.84	3.6	0.90
		SiB2-monthly	0.84	3.5	0.80
		Maize season			
		Coupled model	0.85	4.6	0.89
		SiB2-8day	0.80	5.5	0.83
		SiB2-monthly	0.74	6.3	0.86
	Luancheng	Wheat season			
		Coupled model	0.78	4.7	0.88
		SiB2-8day	0.76	4.9	0.86
		SiB2-monthly	0.69	5.7	0.86
		Maize season			
		Coupled model	0.82	5.6	0.85
		SiB2-8day	0.80	6.0	0.84
		SiB2-monthly	0.67	8.2	0.85

[*] Slope coefficient of linear regression against the observations.

BGD

7, 5157–5190, 2010

Coupling land surface and crop growth models

H. Lei et al.

Table 6. Results of the sensitivity of the model to irrigation amount in the winter wheat season at the Luancheng site (15 October 2007 to 14 June 2008). WUE denotes the water use efficiency (Yield/ET).

Case	*P* (mm)	*I*** (mm)	Max. LAI	SWC*	Yield ($g\,m^{-2}$)	Tr (mm)	ET (mm)	WUE ($kg\,m^{-3}$)
Reality	197	122	6.2	0.26	663	247	365	1.82
1	197	0	5.2	0.18	284	195	311	0.91
2	197	20	6.0	0.19	347	213	327	1.06
3	197	60	6.2	0.22	547	236	349	1.57
4	197	80	6.2	0.24	610	242	356	1.71
5	197	100	6.2	0.25	644	246	361	1.78
6	197	140	6.2	0.27	665	247	365	1.82
7	197	240	6.2	0.28	668	247	366	1.82
8	197	300	6.2	0.28	668	247	366	1.83

* Averaged from 4 Apr to 10 Jun for the root zone
** irrigation was all implemented in 4 Apr 2008.

BGD
7, 5157–5190, 2010
Coupling land surface and crop growth models
H. Lei et al.

Table 7. Simulated impact of increased atmospheric concentration of CO_2 at the Luancheng site.

Crop	$[CO_2]$	Max. LAI	Root-zone SWC	Total biomass carbon ($g\,m^{-2}$)	Tr (mm)	ET (mm)
Wheat**	381 ppm*	6.2	0.253	688	247	365
	762 (2×381) ppm	8.6 (39%)	0.257 (2%)	980 (42%)	233 (−6%)	346 (−5%)
	1143 (3×381) ppm	9.6 (55%)	0.259 (2%)	1093 (59%)	211 (−15%)	327 (−10%)
Maize***	381 ppm*	5.4	0.261	682	210	326
	762 (2×381) ppm	5.6 (4%)	0.272 (4%)	703 (3%)	186 (−11%)	309 (−5%)
	1143 (3×381) ppm	5.7 (6%)	0.280 (7%)	708 (4%)	175 (−17%)	303 (−7%)

* $[CO_2]$ at the current level
** period from 15 Oct 2007 to 14 Jun 2008
*** period from 15 Jun 2008 to 1 Oct 2008
**** Values in the parentheses are relative changes to the current $[CO_2]$ level.

Discussion Paper | Discussion Paper | Discussion Paper | Discussion Paper |

BGD

7, 5157–5190, 2010

Coupling land surface and crop growth models

H. Lei et al.

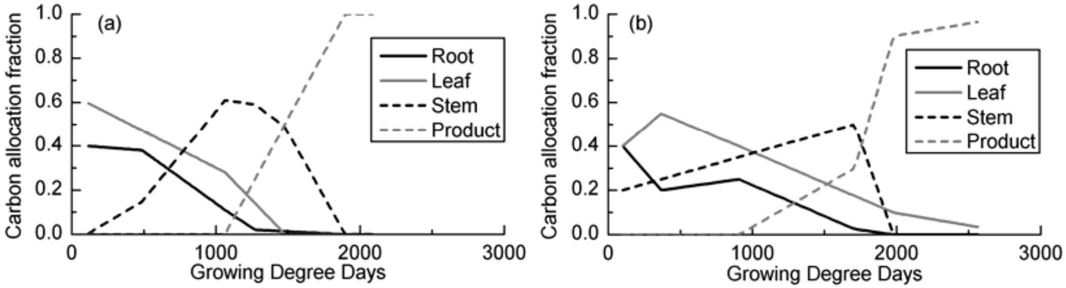

Fig. 1. Carbon allocation scheme for **(a)** winter wheat and **(b)** summer maize.

BGD
7, 5157–5190, 2010

Coupling land surface and crop growth models

H. Lei et al.

Title Page
Abstract | Introduction
Conclusions | References
Tables | Figures
◀| |▶
◀ ▶
Back | Close
Full Screen / Esc
Printer-friendly Version
Interactive Discussion

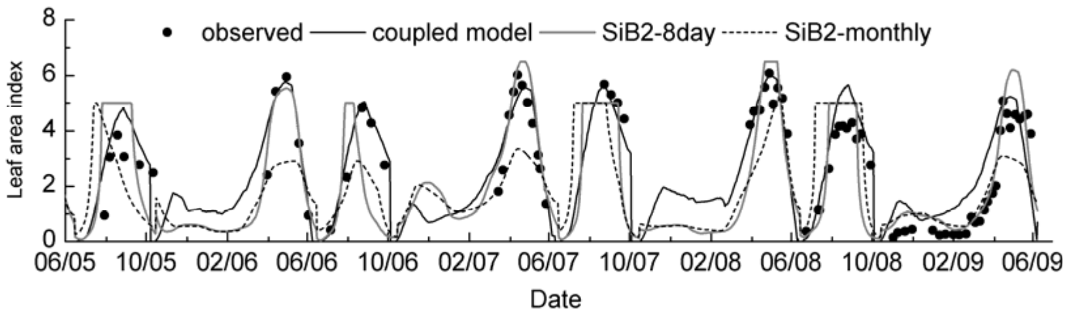

Fig. 2. Simulated and observed leaf area index (LAI) at the Weishan site. The SiB2-8day was derived from eight-day NDVI, and SiB2-monthly was derived from monthly NDVI.

BGD
7, 5157–5190, 2010

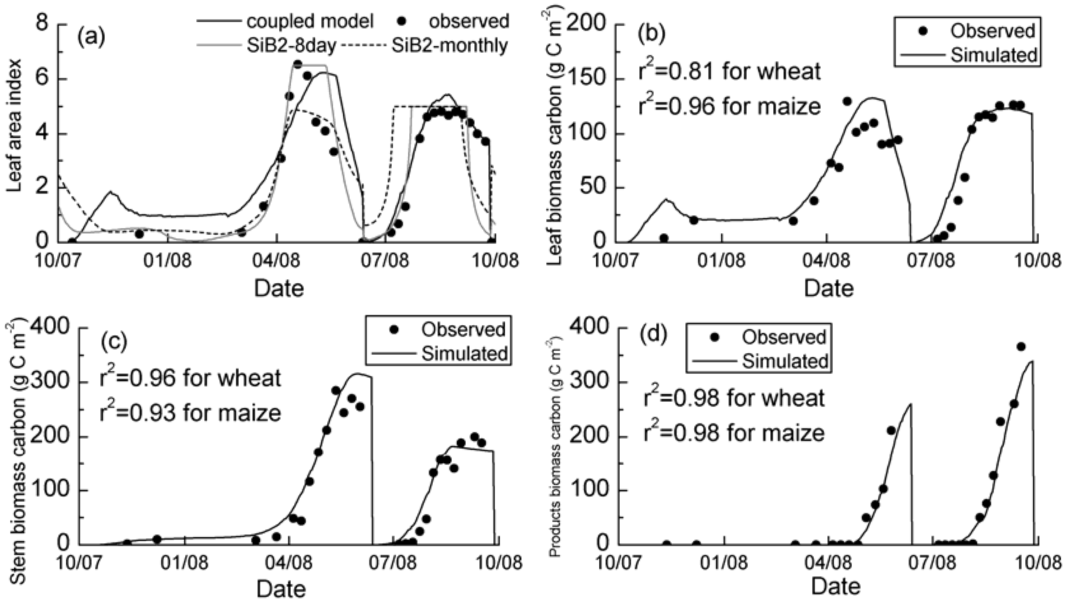

Fig. 3. Simulated and observed **(a)** leaf area index (LAI) and **(b–d)** biomass carbon of different pools at the Luancheng site. r^2 is square of the Pearson product-moment correlation coefficient. In (a), the SiB2-8day was derived from eight-day NDVI and SiB2-monthly was derived from monthly NDVI.

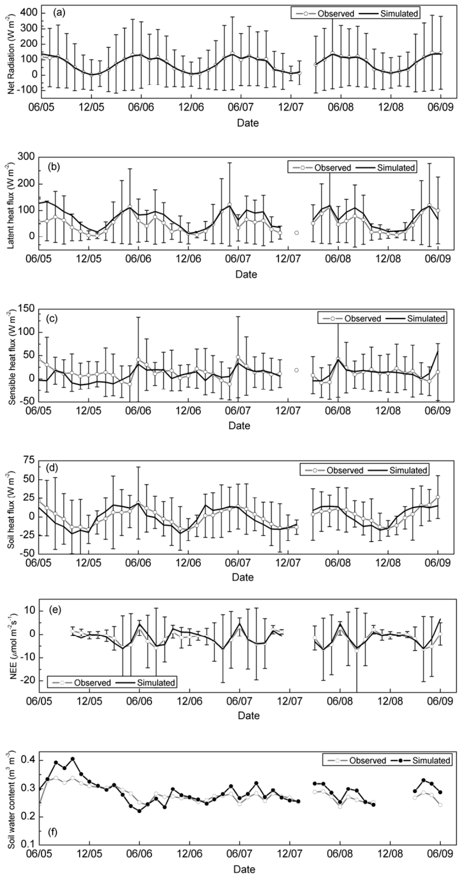

Fig. 4. Seasonal variations in observed and simulated monthly-average values of **(a)** net radiation, **(b)** latent heat flux, **(c)** sensible heat flux, **(d)** soil heat flux, **(e)** net ecosystem exchange (NEE), and **(f)** volumetric soil water content (0–80 cm average) at the Weishan site. Error bars indicate ±1 standard deviation from the mean of the observations.

BGD

7, 5157–5190, 2010

Coupling land surface and crop growth models

H. Lei et al.

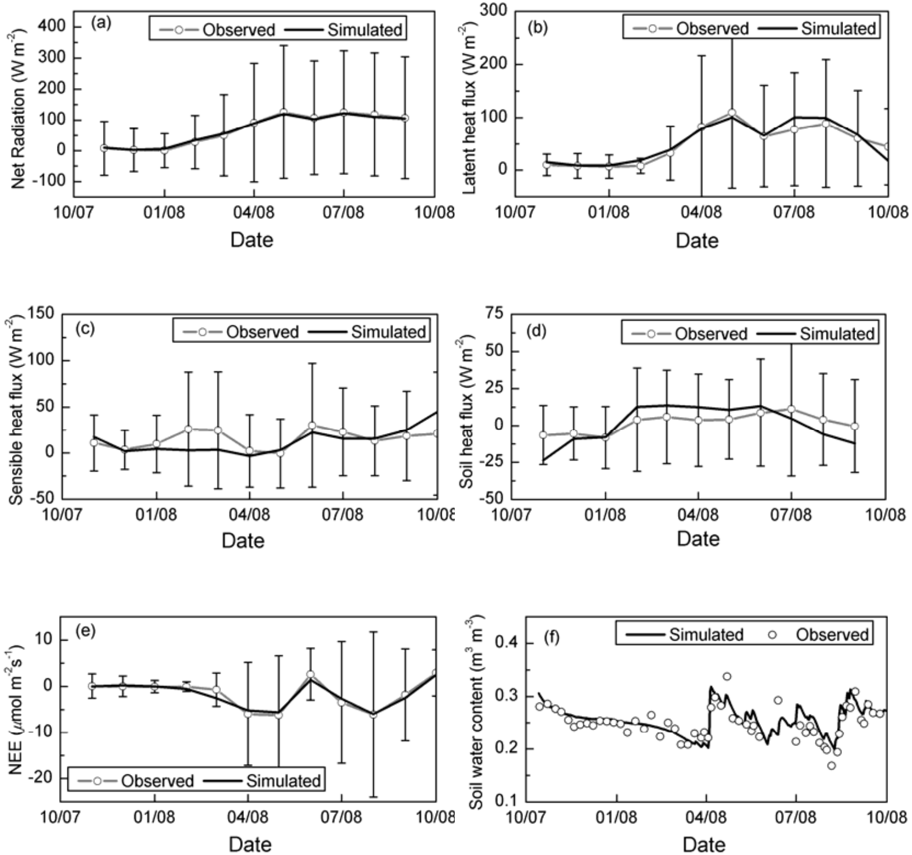

Fig. 5. Seasonal variations in observed and simulated monthly-average values of **(a)** net radiation, **(b)** latent heat flux, **(c)** sensible heat flux, **(d)** soil heat flux, **(e)** net ecosystem exchange (NEE), and **(f)** daily-average volumetric soil water content (0–100 cm average) at the Luancheng site. Error bars indicate ±1 standard deviation from the mean of the observations.

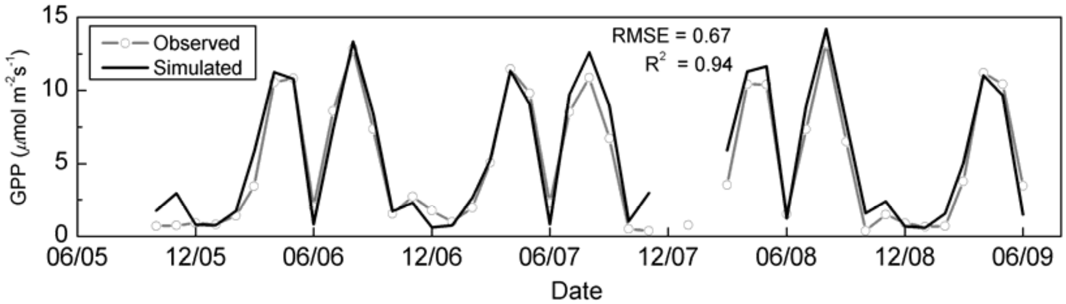

Fig. 6. Simulated and observed monthly-average gross primary production (GPP) at the Weishan site.

BGD
7, 5157–5190, 2010

Coupling land surface and crop growth models

H. Lei et al.

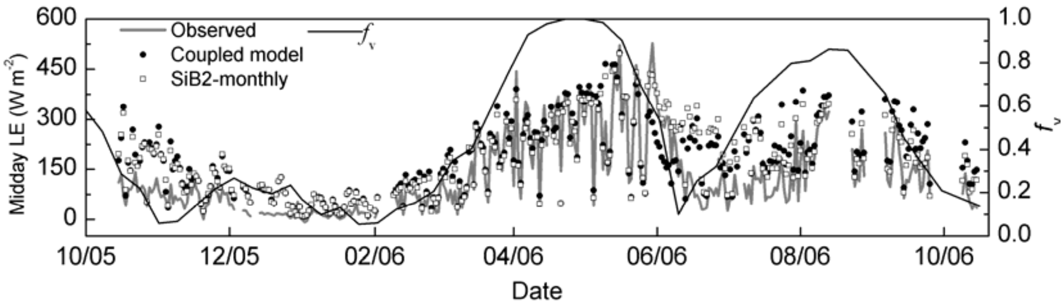

Fig. 7. Midday (10:00–14:00 LT) averaged latent heat flux (LE) from 15 October 2005 to 15 October 2006 at Weishan site. Vegetation cover (f_v) was also presented.

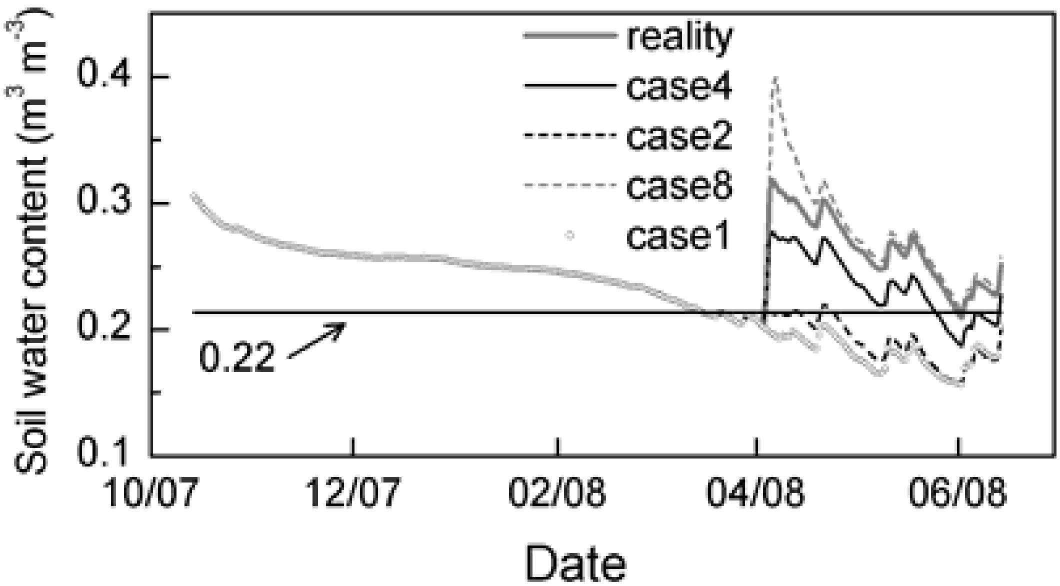

Fig. 8. Simulated root-zone averaged soil water content in different cases. Cases reality, 1, 2, 4, and 8 as given in Table 5, were selected for plotting. The threshold (0.22 m^3 m^{-3}) of incipient soil water stress was also presented.

BGD
7, 5157–5190, 2010

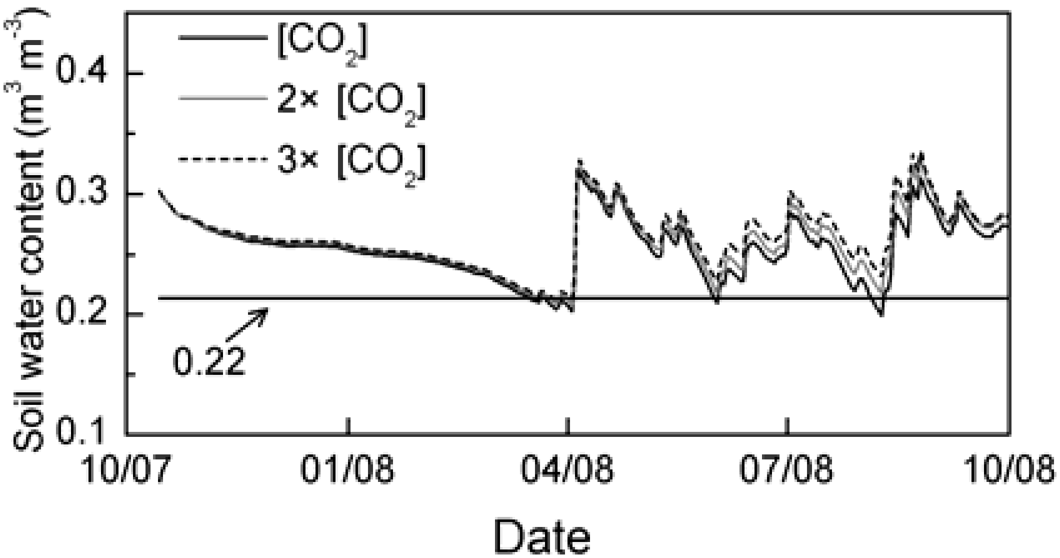

Fig. 9. Simulated root-zone soil water content under different CO_2 concentration levels at the Luancheng site. The [CO_2] denotes 381 ppm, and 0.22 m^3 m^{-3} is the threshold of the incipient water stress.